ISSN 1674-1056
http://cpb.iphy.ac.cn
http://iopscience.iop.org/cpb
中国物理 B
Chinese Physics
中国物理
Chinese Physics B

Impressive self-healing phenomenon of $Cu_2ZnSn(S, Se)_4$ solar cells

Qing Yu(于晴), Jiangjian Shi(石将建), Pengpeng Zhang(张朋朋), Linbao Guo(郭林宝), Xue Min(闵雪), Yanhong Luo(罗艳红), Huijue Wu(吴会觉), Dongmei Li(李冬梅), Qingbo Meng(孟庆波)
Citation: Chin. Phys. B . 2018, 27(6): 066108. **doi:** 10.1088/1674-1056/27/6/066108

Journal homepage: http://cpb.iphy.ac.cn; http://iopscience.iop.org/cpb

What follows is a list of articles you may be interested in

Electronic structure and magnetic properties of (Cu, N)-codoped 3C-SiC studied by first-principles calculations

Feng-chun Pan(潘凤春), Zhi-peng Chen(陈治鹏), Xue-ling Lin(林雪玲), Fu Zheng(郑富), Xu-ming Wang(王旭明), Huan-ming Chen(陈焕铭)
Chin. Phys. B . 2016, 25(9): 096108. **doi:** 10.1088/1674-1056/25/9/096108

Li-ion batteries: Phase transition

Peiyu Hou(侯配玉), Geng Chu(褚赓), Jian Gao(高健), Yantao Zhang(张彦涛), Lianqi Zhang(张联齐)
Chin. Phys. B . 2016, 25(1): 016104. **doi:** 10.1088/1674-1056/25/1/016104

New crystal structure and physical properties of TcB from first-principles calculations

Zhang Gang-Tai, Bai Ting-Ting, Yan Hai-Yan, Zhao Ya-Ru
Chin. Phys. B . 2015, 24(10): 106104. **doi:** 10.1088/1674-1056/24/10/106104

Influences of neutral oxygen vacancies and E_1' centers on α-quartz

Li Hui-Ran, Cheng Xin-Lu, Zhang Hong, Zhao Feng
Chin. Phys. B . 2015, 24(10): 106105. **doi:** 10.1088/1674-1056/24/10/106105

Molecular dynamics simulations of point defects in plutonium grain boundaries

Ao Bing-Yun,Xia Ji-Xing,Chen Pi-Heng,Hu Wang-Yu,Wang Xiao-Lin
Chin. Phys. B . 2012, 21(2): 026103. **doi:** 10.1088/1674-1056/21/2/026103

RAPID COMMUNICATION

Impressive self-healing phenomenon of $Cu_2ZnSn(S, Se)_4$ solar cells*

Qing Yu(于晴)[1,2], Jiangjian Shi(石将建)[1], Pengpeng Zhang(张朋朋)[1,2], Linbao Guo(郭林宝)[1,2], Xue Min(闵雪)[1,2], Yanhong Luo(罗艳红)[1,2], Huijue Wu(吴会觉)[1], Dongmei Li(李冬梅) [1,2,†], and Qingbo Meng(孟庆波)[1,2,‡]

[1] *CAS Key Laboratory for Renewable Energy, Beijing Key Laboratory for New Energy Materials and Devices, Institute of Physics, Chinese Academy of Sciences (CAS), Beijing* 100190, *China*

[2] *School of Physical Sciences, University of Chinese Academy of Sciences, Beijing* 100049, *China*

(Received 4 May 2018; revised manuscript received 11 May 2018; published online 30 May 2018)

A study of the self-healing phenomenon of $Cu_2ZnSn(S, Se)_4$ (CZTSSe) solar cells has shown more than 10% enhancement in cell performance after storage at room temperature for a week, with a significant improvement in the open-circuit photovoltage (V_{oc}) and fill factor (FF). In addition, up to 10.45% power conversion efficiency (PCE) has been achieved. No obvious change in crystallinity, crystal phase, optical absorption or elemental distribution in the CZTSSe films was detected on examining the x-ray diffraction (XRD) pattern, Raman spectrum, ultraviolet-visible (UV-Vis), and TOF-SIMS. Further investigations on the charge carrier concentration, charge radiative recombination, and band structure suggest that the enhancement in PCE stems mainly from a reduction in deep defects of the CZTSSe semiconductor film.

Keywords: $Cu_2ZnSn(SSe)_4$, defects reduction, self-healing

PACS: 61.72.–y, 61.66.Fn, 61.72.Bb **DOI:** 10.1088/1674-1056/27/6/066108

1. Introduction

Recently, thin-film solar cells based on $Cu_2ZnSn(S, Se)_4$ (CZTSSe) light absorbers have attracted wide interest from the scientific as well as industrial community owing to their distinctive advantage of earth abundant composition and low cost. By substituting the In atoms of $Cu(In,Ga)Se_2$ (CIGS) with Zn and Sn atoms a similar lattice structure is retained; therefore, CZTSSe is generally considered as a potential alternative to the conventional chalcopyrite solar cells.[1–3] As a multi-component system,[4] CZTSSe has a large variety of minor phase and lattice defects[5,6] and this complexity hinders an in-depth understanding of the system. Therefore, so far, the highest certified efficiency of this cell is 12.6%,[7] which is much lower than that of the CIGS cells.[8] Therefore, the predecessors made a lot of efforts to understand the CZTSSe system and improved its device efficiency.

During the development of CZTSSe, many important experimental phenomena have been discovered and explored, such as component controlling, Na introducing, and band structure optimization. First, it is the well-known phenomena that Cu-deficient and Zn-rich growth condition yield the highest solar cell efficiency, then subsequent theoretical and experimental studies have shown that this particular composition of CZTSSe can help to reduce deep defects and harmful secondary phases,[6,9] which in turn leads to adjustment of the proportion of the components as $Cu/(Zn+Sn) \approx 0.8$ and $Zn/Sn = 1.1 \sim 1.3$. Second, the fact that devices that use soda-lime glass (SLG) as a base have higher efficiency has attracted attention. Further investigation confirmed that the Na in SLG can diffuse into the absorber and promote crystal growth,[10] increase carrier concentration,[11] and provide grain boundary barriers.[12] These results inspired us to add sodium to the sodium-free flexible substrate and try other similar metal treatments.[13–15] Third, in the early years, a nonuniform Ga/In ratio was found to have a good effect on the CIGS cells. Further studies show that the gradient distribution of these elements can form a gradient band gap, increase light absorption and reduce back surface recombination.[16–18] This concept was also used in CZTSSe and achieved high conversion efficiency.[19,20] Exploring experimental phenomena and applying them in practice is the law of development in a scientific research process.

Here, the phenomenon that the efficiency of the CZTS device can spontaneously increase after storage was observed by many researchers,[21–24] but barely acted upon. We believe that this phenomenon is important and worthy of in-depth research. In this study, systematic experiments were performed to examine the self-healing effect and elucidate its mechanism. By the process of self-healing, the CZTSSe solar cells exhibit over 10% improvement in power conversion efficiency (PCE) after storage at room temperature for a week. This improvement is mainly displayed in a significant enhancement in V_{oc} and FF, besides, up to 10.45% PCE has been achieved. It is found that, for the CZTSSe absorber layer, its trap density

*Project supported by the National Natural Science Foundation of China (Grant Nos. 91733301, 51761145042, 91433205, 11474333, 51421002, 51627803, and 51572288) and the International Partnership Program of the Chinese Academy of Sciences (Grant No. 112111KYSB20170089).

†Corresponding author. E-mail: dmli@iphy.ac.cn

‡Corresponding author. E-mail: qbmeng@iphy.ac.cn

© 2018 Chinese Physical Society and IOP Publishing Ltd

can be significantly reduced after the room-temperature storage whereas the crystallinity, crystal phase, element distribution show no obvious differences. Moreover, this reduction would improve the charge depletion of the CdS/CZTSSe junction and interface energy band bending that would increase the built-in electric field. Based on these positive effects, a self-healing mechanism within the CZTSSe system is suggested, wherein, lattice and atom relaxation or internal stress relaxation driven by the thermodynamics may be possible origins.

2. Experimental section

2.1. Materials

Cu (99.99%), Zn (99.99%), S powder (99.95%, Aladdin), 1,2-ethylenediamine (AR), 1,2-ethanedithiol (AR), cadmium sulfate (AR), and thiourea (AR) were purchased from Aladdin, Sn (99.8%) and Se powders (99.5%) were from Alfa Aesar, and ammonium hydroxide (AR) was from Sinopharm Chemical Reagent Co. Ltd. All the chemicals were directly used as received without further purification.

2.2. Film preparation and device fabrication

The CZTSSe precursor solution with molar ratios of Cu/(Sn+Zn) = 0.74 and Zn/Sn = 1.25 was prepared in accordance with our previous work.[25] Cu (1.65 mmol), Zn (1.23 mmol), Sn (0.98 mmol), S (4 mmol), and Se (0.4 mmol) were dissolved in 5-mL 1, 2-ethylenediamine and 0.5-mL 1, 2-ethanedithiol. The mixture was continuously stirred for 1.5 h at 90 °C to give a clear yellow solution. The precursor solution was spin-coated at 5000 rpm onto Mo-coated soda lime glass and heated on a hot plate at 380 °C for 1 min. The same process was repeated several times to produce a precursor film of about 1.5-μm thickness which was then selenized under Se/N_2 atmosphere at 550 °C in a graphite box for 15 min to get the required CZTSSe film.

An SLG/Mo/CZTSSe/CdS/ZnO/ITO/Ag solar cell was prepared by successively depositing a CdS buffer by chemical bath method, radio frequency (RF) magnetron sputtered ZnO combined with indium tin oxide (ITO) window layers, and evaporated Ag collection grid. The active area of each device for *J–V* measurement was 0.18 cm^2.

2.3. Characterization

For characterization, the as-prepared CZTSSe film or device was labelled as "*x* d" which represents samples of the same batch stored for *x* days, for example, "0 d" is the sample without storage and "7 d" is that of the same batch stored in dark conditions for 7 days. These 7-d samples were sealed by a vacuum compressor under a rough vacuum and stored at room temperature. The current density–voltage (*J–V*) characterization for the solar cells was performed under AM1.5 illumination (1000 $W{\cdot}m^{-2}$) using an Xe-based light source solar simulator (Zolix SS150A), calibrated by a standard Si reference cell. The x-ray diffraction (XRD) was performed by using an x-ray diffractometer with Cu Kα as the radiation source (Empyrean, PANaltical). Raman spectra were collected by a Raman spectrometer (HR800, Jobin Yvon), using a 532-nm excitation laser with a power of 0.1 mW. The compositional depth profile was obtained by secondary-ion mass spectroscopy (TOF-SIMS 5, Germany ION-TOF GmbH), samples were CZTSSe and standard CdS films on Mo/SLG, 20-kV ion energy and 13.7-nA ion current was employed for analysis throughout the film, 5-kV ion energy and 4-nA ion current was used to analyze a superficial zone of CdS. The capacitance–voltage (*C–V*) and drive-level capacitance profile (DLCP) characterizations were measured on an electrochemical workstation (Versa STAT3, Princeton). The *C–V* data was performed at 100 kHz and 50-mV alternating current (AC) excitation source with direct current (DC) bias ranging from 0.5 V to −1.0 V, and the DLCP measurement was performed on 100 kHz while changing the AC perturbation voltage from 20 mV to 140 mV and DC bias from 0.5 V to −1.0 V. The band gap of the samples was determined by UV-Vis-NIR spectra on UV-3600 spectrophotometer, Shimadzu and steady-state PL spectra were obtained from a fluorescence spectrometer (FLS920, Edinburgh Instruments) with the time integration mode. The film was excited by a 535-nm monochromatic light from a xenon lamp. The valence band information was investigated via x-ray photoelectron spectroscopy (XPS) (ESCALAB 250X, Thermo Fisher Scientific) using a monochromatic Al Kα source of energy 1486.6 eV. The samples were charge-neutralized using an in-lens electron source combined with a low-energy (1 eV) Ar+ flood source. The samples for XPS characterization were as follows: "CZTSSe" sample was a fresh absorber layer, "CdS" sample was standard CdS (CBD for 11 min) deposited on CZTSSe base, "CZTSSe/CdS" sample was ultrathin CdS (CBD for 2 min) depositing on CZTSSe, which allowed the x-rays to penetrate the thin CdS to investigate both the thin CdS layer and the CZTSSe layer.

2.4. Theoretical calculation of the band alignment of the cell

The carrier distribution and electric field inside the cell were theoretically calculated by solving the Poisson's equations charge conservation and continuity equations in the dark by a general device simulator Analysis of Microelectronic and Photonic Structures (AMPS-1D). Dielectric constant 8.1 for CZTSSe, 9 for CdS, 7.8 for ZnO; defect densities of 10^{17} cm^{-3} and 10^{16} cm^{-3} were the values used to calculate the band alignments for 0 d and 7 d.

3. Results and discussion

3.1. Systematic experiments

As shown in Fig. 1(a), after being stored at room temperature for a week, the average efficiency of the CZTSSe solar cell exhibits an obvious increase indicating that the solar cells have been self-healed. Figure 1(b) shows that the solar cell efficiency does not decrease even after 110 days, suggesting that the self-healing effect is stable and irreversible. In order to find the origin of this phenomenon, systematic experiments were performed. At first, the influence of different atmospheres on the efficiency evolution was studied. As shown in Fig. 1(c), whether in air or Ar atmosphere, the average efficiency of the cells increased similarly by about 0.7%, thus suggesting that oxygen is not responsible for the self-healing process.[26] Moreover, a similar phenomenon is observed when the cell is stored in vacuum. This performance enhancement is thus suggested to be attributed to the device itself.

It is widely reported that the Na diffusion within the CZTSSe film, usually introduced by post-annealing,[27–29] could help to improve the device performance. Relevant contrast experiments were also carried out to resolve this influence. For comparison, the CZTSSe films were fabricated on the quartz substrate (without Na).[30] Time-dependent current–voltage (J–V) results of the quartz substrate-based cell as well as that of the general soda-lime glass (SLG) are given in Fig. 1(d). It can be seen that, the standard SLG-based cell exhibits an obvious improvement in efficiency after seven days of storage, and a high efficiency up to 10.45% is obtained. Although the efficiency of the quartz-based cells is much lower than that of the SLG one, an improvement is observed in its performance as well. The quartzbased solar cell exhibits a level of performance growth similar to the SLG solar cell, indicating that Na diffusion is not the origin for self-healing. Thus, in the following sections, we mainly focus on the SLG-based cell.

Table 1 gives the statistical results of the performance parameters from 65 cells (the corresponding statistical histogram is shown in Fig. S1 in Appendix A). We can see that, after 7 days, the average efficiency of the devices increases from

Table 1. Statistical result of the electrical properties of the cells (65 cells). R_S, R_{SH}, A, and J_0 are the series resistance, shunt resistance, ideality factor, and reverse saturation current determined from light J–V data referenced Steven S Hegedus method.[31]

	Efficiency/%	J_{sc}/mA·cm^{-2}	V_{oc}/mV	FF	R_S/Ω·cm^2	R_{SH}/kΩ·cm^2	A	J_0/mA·cm^{-2}
0 d	8.03 ± 0.93	32.04 ± 1.40	432.2 ± 24.8	0.58 ± 0.05	0.98 ± 0.52	249 ± 140	2.08 ± 0.24	$(2.1 \pm 2.8) \times 10^{-2}$
7 d	9.08 ± 0.65	32.26 ± 1.10	461.2 ± 19.6	0.64 ± 0.02	1.11 ± 0.44	472 ± 240	1.76 ± 0.20	$(2.2 \pm 1.7) \times 10^{-3}$

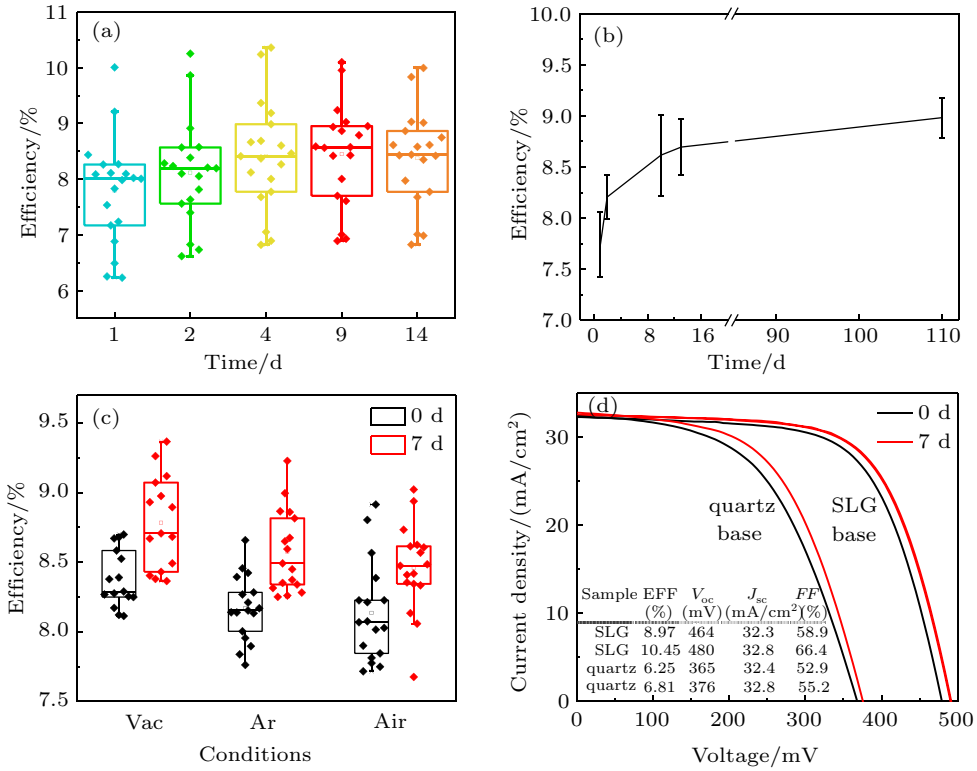


Fig. 1. (color online) (a) Photoelectric conversion efficiency evolution of baseline devices. (b) Device efficiency stability from initial fabrication to 110-days remeasurement. (c) Photoelectric conversion efficiency changes of baseline devices by seven-day storage in different conditions: rough vacuum, argon atmosphere and air. (d) Time-dependent light current–voltage (J–V) of the baseline SLG base sample and quartz base sample.

8.03% to 9.08%, by about 13%. Obviously, this improvement mainly comes from the increase in V_{oc} (from 432.2 mV to 461.2 mV) and the FF (from 0.58 to 0.64), whereas the short-circuit current densities (J_{sc}) are similar to each other. As the energy bandgap E_g, (Fig. 3(b)) remains unchanged in the storage process, this improvement in V_{oc} directly indicates a decrease in the V_{oc} deficit. This implies that the performance enhancement could arise from the suppression of charge recombination.[31] According to the charge transfer model of a heterojunction, the electrical properties of these cells have been further derived from their J–V curves.[31] The series resistance (R_S), slightly increases from 0.98 $\Omega\cdot cm^2$ to 1.11 $\Omega\cdot cm^2$, implying that the charge transport capability of the CZTSSe film and the interfaces, especially of the CZTSSe/Mo interface, has not improved. On the other hand, the shunt resistance (R_{SH}) is significantly enhanced from 249 $k\Omega\cdot cm^2$ to 472 $k\Omega\cdot cm^2$, which in theory could directly lead to the increase in V_{oc} and FF. This improvement may arise from (i) partial elimination of high-conductive secondary phases, such as $Cu_2(S, Se)$ and $Cu_2Sn(S, Se)_3$, within the CZTSSe film or (ii) the charge recombination suppression.[5,32] The reduction in the charge recombination is further supported by the decreased ideality factor (A) of the heterojunction. For the as-prepared cell, A is about 2.08, almost the same as that of the theoretical value ($A = 2$) indicating the recombination mechanism dominating in the junction region. After 7 days, the value of A is reduced to 1.76, suggesting that the charge diffusion mechanism also participates in determining the charge transfer within the cell, which is mainly caused by the decrease in the charge recombination. The calculation of the inverse saturated current density (J) directly supports this result. As shown in Table 1, after 7 days, the J of the cell decreases from 2.1×10^{-2} $mA\cdot cm^{-2}$ to 2.2×10^{-3} $mA\cdot cm^{-2}$, by about one order of magnitude. It can be thus verified that the charge recombination within the CZTSSe absorber, especially in the junction region, has been significantly suppressed.

3.2. Characterizations on crystallinity, crystal phase and elements distribution

For a CZTSSe solar cell, its charge recombination is influenced by many aspects, such as the crystallization, secondary phase, element distribution and defect density.[5,32,33] First, the XRD pattern and Raman spectra are used to study the possible phase evolution during the storage. As seen in Fig. 2(a), almost no difference in XRD patterns can be distinguished even after 7 days' storage. The diffraction peaks at 17.5°, 27.4°, 36.4°, 45.6°, and 54.1° are assigned to the [011], [112], [211], [220]/[204], and [312]/[116] planes of the CZTSSe lattice,[34,35] respectively, and no obvious secondary phase peak is observed. As illustrated in Fig. 2(b), the Raman spectra shows a strong peak at 198 cm^{-1}, which is close to the A mode of kesterite CZTSe at 196 cm^{-1}.[36] Being similar to the results of XRD, no minor phases like $Cu_2(S, Se)$ or $Cu_2Sn(S, Se)_3$ are observed and the spectra are unchanged

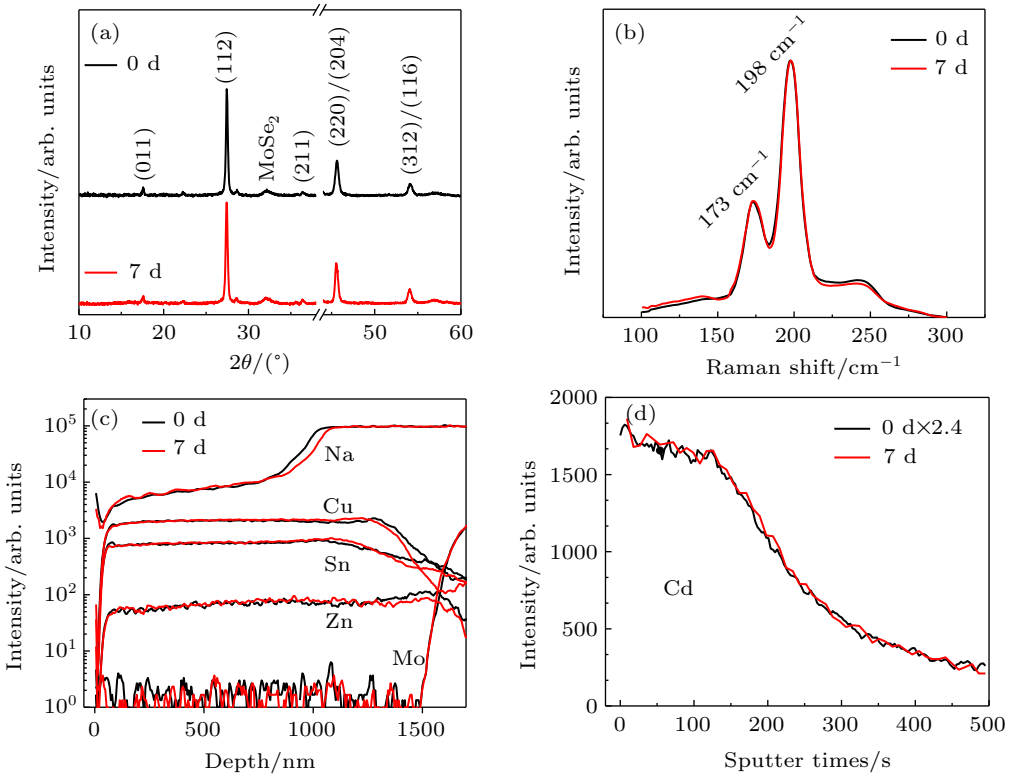


Fig. 2. (color online) (a) Time-dependent XRD pattern of CZTSSe absorber film. (b) Normalized Raman spectra of CZTSSe absorber films. SIMS depth profile of (c) Na, Cu, Zn, Sn content throughout the film (d) Cd content of superficial area, the 0-d sample intensity multiplied by 2.4 times.

after storage. In addition, top-view scanning electron microscope (SEM) images in Figs. S2(a) and S2(b) of Appendix A also show no difference with time. All these results infer that the crystallization and phase of the CZTSSe film has not changed with time. Besides, the Raman spectrum and band gap have also been used to characterize the Cu/Zn disorder within the CZTSSe lattice.[37,38] The identical Raman spectrum and unchanged band gap (Fig. 3(b)) indicate that the Cu/Zn disorder also experiences no change with time. The element distribution within the cell is probed by a TOF-SIMS measurement. The depth of it is calibrated by the Mo signal and film thickness acquired from a cross-sectional SEM image as shown in Fig. S2(c). We can see from Fig. 2(c) that the distribution of the metal elements does not change with time, and the distribution of S and Se in Fig. S3 of Appendix A show little change as well. Therefore, the possibility of an exhausted Cu surface is also excluded.[39,40] For the CZTSSe, it is generally considered that the diffusion of the impurity atoms, such as the Na from the SLG substrate and Cd from the buffer layer, could help to passivate some defects and thus promote the device performance.[29,41,42] However, as shown in Figs. 2(c) and 2(d), the Na and Cd distribution within the CZTSSe film is unchanged, suggesting that further longitudinal diffusion of these elements does not happen in the self-healing process. Based on the above measurements, we can conclude that the performance enhancement of the cell after storage is not due to the change in the phase, Cu/Zn ordering, crystalline or element distribution.

3.3. Characterizations on defects and energy bands

The DLCP and *C–V* measurements[43,44] have been conducted to evaluate defect properties of the CZTSSe absorber. To exclude the possible influence from other layers, the same batch of Mo/CZTSSe films is selected for the following measurement. In this batch, the samples are classified into two parts, defined as 0-d and 7-d samples, respectively, and one part was directly fabricated into the device without any storage while the other was stored for 7 days and then fabricated into the devices by following the same process. As shown in Fig. 3(a), after 7 days, the charge-carrier density within the film is significantly reduced by about one order of magnitude (from 10^{17} cm^{-3} to 10^{16} cm^{-3}), indicating an obvious reduction in defects, even though it cannot be determined whether these are shallow or deep defects. For 0-d sample, a high charge density of about 10^{17} cm^{-3} is estimated by both the DLCP and *C–V* measurements, suggesting that a large number of bulk defects could exist within the as-prepared CZTSSe film, thus resulting in a narrow charge depletion region with a width (W_D) of only about 140 nm. For the 7-d cell, as the charge-carrier density decreased, the W_D is subsequently extended to 240 nm, which could effectively facilitate photocarrier transportation.

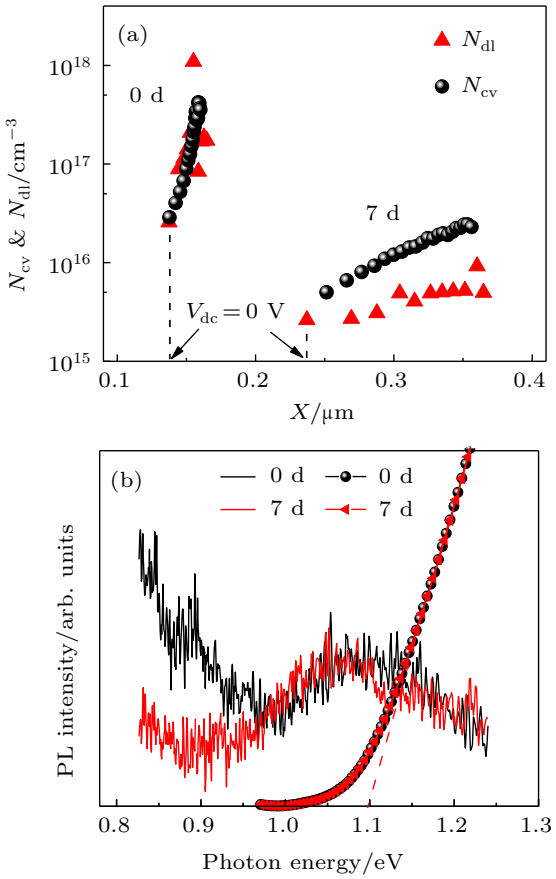


Fig. 3. (color online) (a) Comparison of the time-dependent charge carrier densities in the CZTSSe absorber film solar cells at 300 K determined by *C–V* (N_{cv}) and DLCP (N_{dl}). The dashed line indicates the depletion width at 0-V bias. (b) Photoluminescence (PL) spectrum and Tauc plots calculated from ultraviolet–visible measurements of CZTSSe absorber films before and after storage.

Steady-state photoluminescence spectroscopy (PL) has been further employed to investigate bulk defects in the CZTSSe film. The CZTSSe film was covered by a PMMA layer (∼ 200 nm) to prevent the surface from the external atmosphere (such as oxygen and water). As shown in Fig. 3(b), for the as-prepared 0-d CZTSSe film, two irradiative emission bands, a continuum-band emission at 1.08 eV (∼ 1149 nm) and a defect emission at below 0.85 eV, can be distinguished. The position of the continuum-band emission agrees well with the E_g (1.1 eV) derived from the light absorption curve, implying that no obvious emission red-shift was caused by band-tail states in the CZTSSe system.[45] Owing to limited measurement range of the instrument, we could not obtain its full spectrum. However, it could still be ascertained that this defect was deeper than Cu_{Zn} or V_{Cu} which could provide free carriers in CZTSe, and further, these deep defects may be Sn-related or S/Se vacancy defects.[6] For the 7-d CZTSSe film, the E_g and continuum-band emission are similar to that of the 0-d one, while the deep-defect emission is significantly suppressed. This implies that these defect states have been significantly passivated, in line with the DLCP and *C–V* results. In view of the above observations, it is suggested that the perfor-

mance improvement of the cell with extended storage time is mainly due to the reduction of these deep defects.

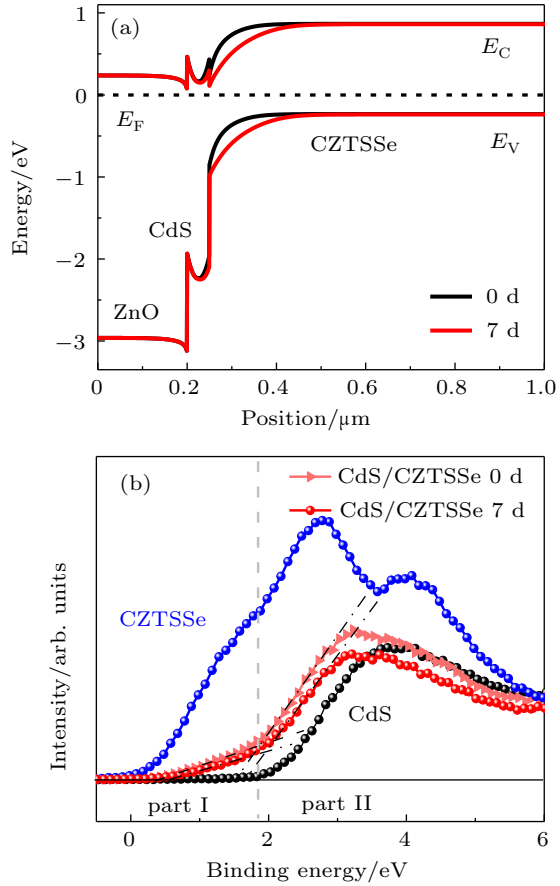


Fig. 4. (color online) (a) Band alignments theoretically simulated by AMPS-1D with different defect densities (1×10^{17} cm^{-3} for "0 d", 1×10^{16} cm^{-3} for "7 d"). (b) XPS measured valence band spectrum of CZTSSe sample, CdS sample and the 7-days change of several nanometers coated CZTSSe film (CdS/CZTSSe sample). The black dot lines are only guides for the eye and indicate the approximate VBM positions, according to the linear extrapolation method. The spectra of CdS/CZTSSe sample is divided by the zero point of CdS sample's density of states, named part I and part II.

To further confirm the above assumption, the influence of the reduction in the deep-defect density on the electric properties of the cell has been studied by theoretical simulation on the band alignment.[46,47] As shown in Fig. 4(a), when the defect density decreases from 10^{17} cm^{-3} to 10^{16} cm^{-3}, the W_D is obviously extended as expected. Moreover, the simulation indicates that the band bending properties at the interface are different for these two conditions. For the low-defect-density cell, the energy difference between the Fermi energy level and the valence band of the CZTSSe is obviously increased, implying that band bending is enhanced. Experimentally, this energy difference has been probed by the XPS valence-band spectroscopy. Figure 4(b) gives the XPS valence-band spectra of the 0-d and 7-d CdS/CZTSSe samples, where the CdS is ultrathin to make the CZTSSe detectable. The core levels of both $Sn^{3\,d}$ and $Cd^{3\,d}$ in the CdS/CZTSSe sample are shown in Fig. S4 of Appendix A. The spectra of CdS/CZTSSe sample can be separated into two parts, as depicted in Fig. 4(b). The low-energy tail (part I) is ascribed to the CZTSSe while the high-energy shoulder (part II) to both the CdS and CZTSSe. It can be found that the valence-band edge variation of part I (from 0.39 eV to 0.54 eV) is close to that of part II (from 1.50 eV to 1.66 eV), suggesting that the change of the CdS/CZTSSe sample is caused by the common CZTSSe layer. No obvious change in the valence-band spectrum of CdS sample after storage is found to support this result, as shown in Fig. S4(c). Besides, the 150-meV down-shift of the valence band is in good agreement with the theoretical prediction, which signifies an increased built-in electric field.

In view of the above discussion, it is suggested that the deep defects, like Sn-related or S/Se vacancy defects, in the CZTSSe absorber layer are spontaneously reduced after storage at room temperature. This reduction could help to suppress charge recombination, and furthermore lead to a wider depletion and a stronger built-in electric field. Therefore, V_{oc} and FF significantly increase after the self-healing and lead to better device performance. This improvement may be attributed to: i) the atomic relaxation in grain boundary (GB) regions.[48] The dangling bonds at the GB create localized defect states,[49,50] and the nanoscale horizontal diffusion of atoms is undetectable by SIMS, but can break or weaken the detrimental dangling bonds thus eliminating the deep gap states; ii) the release of internal stress within the CZTSSe film. The compressive internal stress in the asprepared film[51] is spontaneously released at room temperature,[52] which helps to optimize the spatial energy band distribution and thus reduce the charge localization centers. This self-healing effect presents a valuable opportunity to recognize the hidden mechanism that was limiting the device performance.

4. Conclusion and perspectives

An impressive self-healing effect of the defects within the CZTSSe absorber is observed, which significantly contributes to the performance enhancement of the solar cell. No obvious changes are found in the crystalline, phase, element composition, or impurity atom diffusion of the CZTSSe film. Further investigation reveals that this effect is mainly assigned to a significant reduction in the deep defect density of the CZTSSe semiconductor, and the relevant physics mechanism behind this behavior has been investigated. Spontaneous passivation of dangling bonds at the grain boundaries and the release of local stress within the CZTSSe at room temperature could be possible reasons for this reduction in the deep defect density. This interesting self-healing effect and the physics mechanism involved therein provide an opportunity to further understand the performance-limited mechanisms of CZTSSe devices, which has great values for the device optimization and performance enhancement.

Appendix A: Supplementary material

Some supporting materials for better understanding this paper are provided in the following figures.

As shown in Fig. S1, a significantly improvement in solar cell efficiency is obtained after 7-days storage. Obviously, this improvement mainly displays in the increase in V_{oc} and the FF, whereas the short-circuit current densities (J_{sc}) just improve a little. This result indicates the recombination may be suppressed during the self-healing process.[31]

Top-view SEM image in Figs. S2(a) and S2(b) shows the well-crystallized CZTSSe layer. For the 0-d and 7-d samples, no obviously different is observed indicating the crystallization has not changed with time, which is consistent with XRD results. The cross-sectional SEM image in Fig. S2(c) shows this CZTSSe thin film exhibits a typical bi-layer structure (large-grain layer and finegrain layer). The total thickness of this CZTSSe film is about 1.7 μm, while the thickness of large-grain layer is about 0.9 μm. The same sample was used for SIMS characterization.

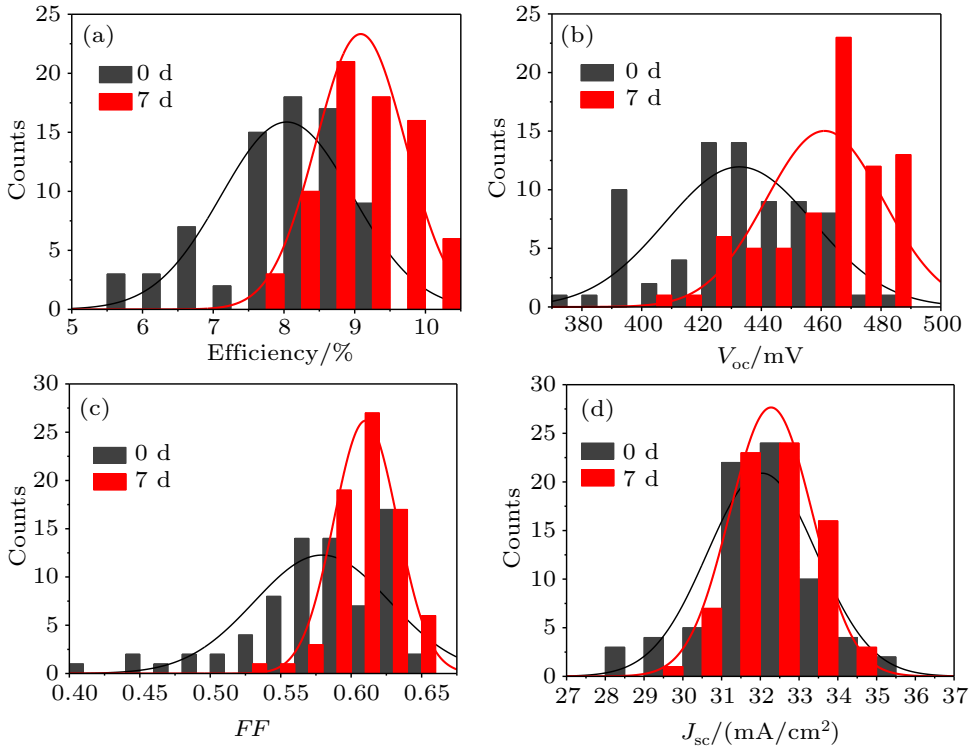


Fig. S1. (color online) Statistic results of (a) efficiency, (b) open-circuit voltage, (c) fill factor, (d) short-circuit current for 65 cells.

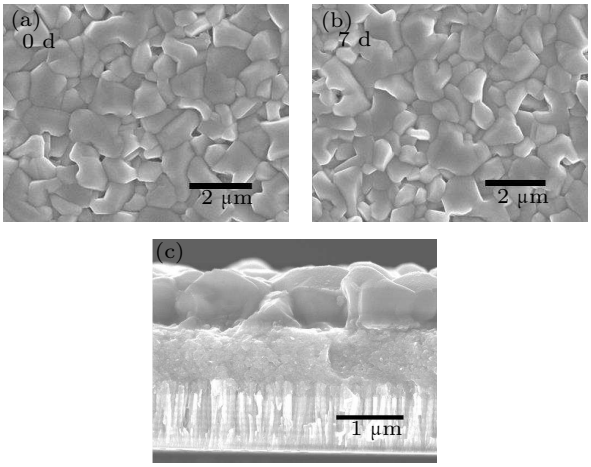


Fig. S2. Top-view SEM image of CZTSSe absorber film (a) before and (b) after storage. (c) Cross-sectional SEM image of SIMS sample.

As shown in Fig. S3, Se element distributes uniformly throughout the film, while the content of S element in the small grain layer is slightly lower than that in the large grain layer. But both of the two elements change little after storage.

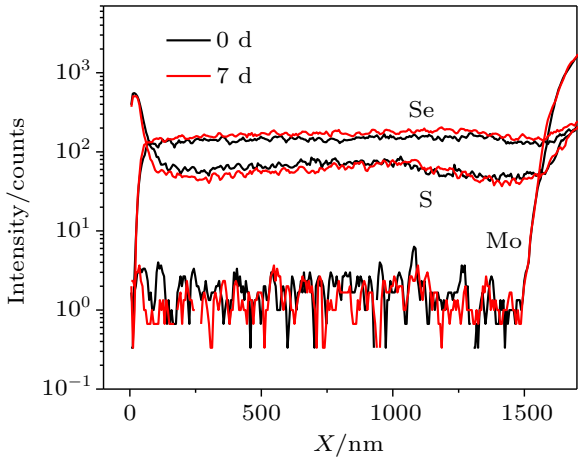


Fig. S3. (color online) SIMS depth profile of S and Se content throughout the film.

CdS/CZTSSe sample is the ultrathin CdS coated

CZTSSe, which is attempt to make both the CZTSSe and CdS detectable. The core levels of Sn^{3d} and Cd^{3d}, shown in Figs. S4(a) and S4(b), are from the CZTSSe layer and CdS layer, respectively, indicating the signal of the two layers is reliably detected. Besides, the core levels' binding energy of the two elements coincide well at 0 day and 7 days, indicating that the valence band movement of CdS/CZTSSe sample is not caused by the test error.

The overlapping valence bands of CdS samples demonstrate that the valence band shift of the CdS/CZTSSe sample is due to the change of the CZTSSe layer.

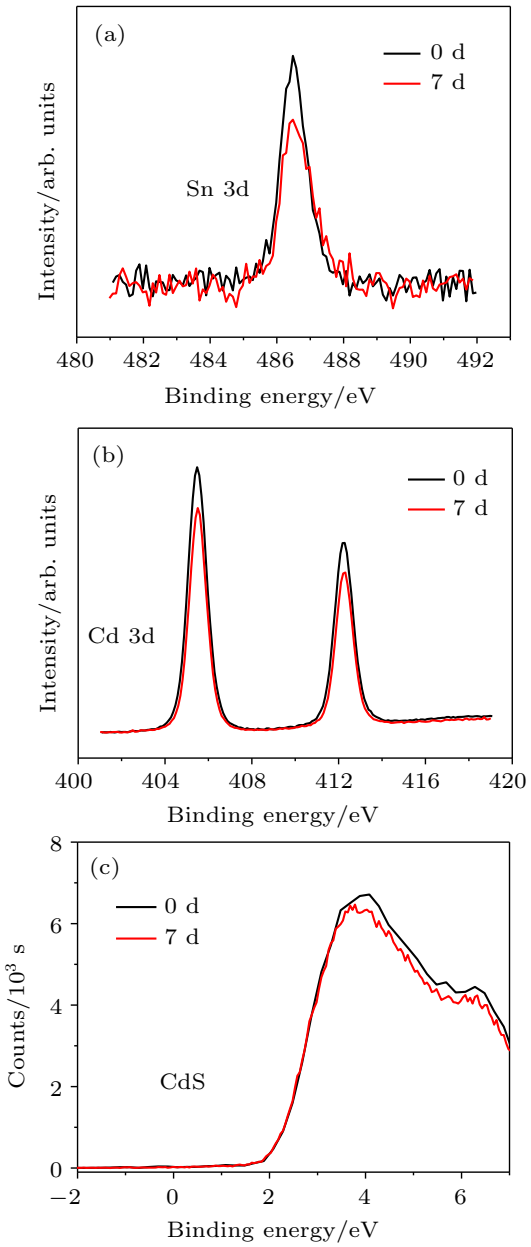


Fig. S4. (color online) The CdS/CZTSSe sample's core levels of (a) Sn^{3d} and (b) Cd^{3d}. (c) Valence band spectrum of CdS sample before and after storage.

References

[1] Polizzotti A, Repins I L, Noufi R, Wei S H and Mitzi D B 2013 *Energy Environ. Sci.* **6** 3171

[2] Walsh A, Chen S, Wei S H and Gong X G 2012 *Adv. Energy Mater.* **2** 400

[3] Mitzi D B, Gunawan O, Todorov T K, Wang K and Guha S 2011 *Sol. Energy Mater. Sol. Cells* **95** 1421

[4] Liu D, Han D, Huang M, Zhang X, Zhang T, Dai C and Chen S 2018 *Chin. Phys. B.* **27** 018806

[5] Altamura G and Vidal J 2016 *Chem. Mater.* **28** 3540

[6] Chen S, Walsh A, Gong X G and Wei S H 2013 *Adv. Mater.* **25** 1522

[7] Wang W, Winkler M T, Gunawan O, Gokmen T, Todorov T K, Zhu Y and Mitzi D B 2014 *Adv. Energy Mater.* **4** 1301465

[8] Jackson P, Wuerz R, Hariskos D, Lotter E, Witte W and Powalla M 2016 *Phys. Status Solidi Rapid Res. Lett.* **10** 583

[9] Min X, Shi J J, Guo L B, Yu Q, Zhang P P, Tian Q W, Li D M, Luo Y H, Wu H J, Meng Q B and Wu S X 2018 *Chin. Phys. B* **27** 016402

[10] Hlaing Oo W M, Johnson J L, Bhatia A, Lund E A, Nowell M M and Scarpulla M A 2011 *J. Electron. Mater.* **40** 2214

[11] Prabhakar T and Jampana N 2011 *Sol. Energy Mater. Sol. Cells* **95** 1001

[12] Li J B, Chawla V and Clemens B M 2012 *Adv. Mater.* **24** 720

[13] López-Marino S, Sánchez Y, Espíndola-Rodríguez M, Alcobé X, Xie H, Neuschitzer M, Becerril I, Giraldo S, Dimitrievska M, Placidi M, Fourdrinier L, Izquierdo-Roca V, Pérez-Rodríguez A and Saucedo E 2016 *J. Mater. Chem. A* **4** 1895

[14] Xin H, Vorpahl S M, Collord A D, Braly I L, Uhl A R, Krueger B W, Ginger D S and Hillhouse H W 2015 *Phys. Chem. Chem. Phys.* **17** 23859

[15] Chen F S, Sung J C, Yang C Y and Lu C H 2015 *J. Nanomater.* **2015** 579510

[16] Dullweber T, Lundberg O, Malmstrom J, Bodegard M, Stolt L, Rau U, Schock H W and Werner J H 2001 *Thin Solid Films* **387** 11

[17] Dullweber T, Hanna G, Rau U and Schock H W 2001 *Sol. Energy Mater. Sol. Cells* **67** 145

[18] Gloeckler M and Sites J R 2005 *J. Phys. Chem. Solids* **66** 1891

[19] Qi Y F, Kou DX, Zhou W H, Zhou Z J, Tian Q W, Meng Y N, Liu X S, Du Z L and Wu S X 2017 *Energy Environ. Sci.* **10** 2401

[20] Yang K J, Son D H, Sung S J, Sim J H, Kim Y I, Park S N, Jeon D H, Kim J, Hwang D K, Jeon C W, Nam D, Cheong H, Kang J K and Kim D H 2016 *J. Mater. Chem. A* **4** 10151

[21] Meng Q B 2017 Personal discussion on "The first copper-based thin film solar cell seminar"

[22] Antunez P D, Bishop D M, Luo Y and Haight R 2017 *Nat. Energy* **2** 884

[23] Colina M, Bailo E, Medina-Rodríguez B, Kondrotas R, Sánchez-González Y, Sylla D, Placidi M, Blanes M, Ramos F, Cirera A, Pérez Rodríguez A and Saucedo E 2018 *J. Alloys Compd.* **735** 2462

[24] Collord A D and Hillhouse H W 2016 *Chem. Mater.* **28** 2067

[25] Zhang P P, Yu Q, Min X, Guo L B, Shi JJ, Zhao X Y, Li D M, Luo Y H, Wu H J, Meng Q B, Wu S X 2018 *RSC Adv.* **8** 4119

[26] Cahen D and Noufi R 1989 *Appl. Phys. Lett.* **54** 558

[27] Cadel E, Barreau N, Kessler J and Pareige P 2010 *Acta Mater.* **58** 2634

[28] Shin D, Kim J, Gershon T, Mankad R, Hopstaken M, Guha S, Ahn B T and Shin B 2016 *Sol. Energy Mater. Sol. Cells* **157** 695

[29] Hironiwa D, Sakai N, Kato T, Sugimoto H, Tang Z, Chantana J and Minemoto T 2015 *Thin Solid Films* **582** 151

[30] Yang Y, Huang L and Pan D 2017 *ACS Appl. Mater. Interfaces* **9** 23878

[31] Hegedus S S and Shafarman W N 2004 *Prog. Photovoltaics: Res. Appl.* **12** 155

[32] Huang T J, Yin X S, Qi G J and Gong H 2014 *Phys. Status Solidi-Rapid Res. Lett.* **8** 735

[33] Bourdais S, Chone C, Delatouche B, Jacob A, Larramona G, Moisan C, Lafond A, Donatini F, Rey G, Siebentritt S, Walsh A and Dennler G 2016 *Adv. Energy Mater.* **6** 1502276

[34] Li J, Wang H, Luo M, Tang J, Chen C, Liu W, Liu F, Sun Y, Han J and Zhang Y 2016 *Sol. Energy Mater. Sol. Cells* **149** 242

[35] Guo J, Zhou W H, Pei Y L, Tian Q W, Kou D X, Zhou Z J, Meng Y N and Wu S X 2016 *Sol. Energy Mater. Sol. Cells* **155** 209

[36] Nam D, Kim J, Lee J U, Nagaoka A, Yoshino K, Cha W, Kim H, Hwang I C, Yoon K B and Cheong H 2014 *Appl. Phys. Lett.* **105** 173903

[37] Rey G, Redinger A, Sendler J, Weiss T P, Thevenin M, Guennou M, El Adib B and Siebentritt S 2014 *Appl. Phys. Lett.* **105** 112106

[38] Scragg J J S, Choubrac L, Lafond A, Ericson T and Platzer-Björkman C 2014 *Appl. Phys. Lett.* **104** 041911

[39] Chirila A, Reinhard P, Pianezzi F, Bloesch P, Uhl A R, Fella C, Kranz L, Keller D, Gretener C, Hagendorfer H, Jaeger D, Erni R, Nishiwaki S, Buecheler S and Tiwari A N 2013 *Nat. Mater.* **12** 1107

[40] Gao S, Zhang Y, Ao J, Li X, Qiao S, Wang Y, Lin S, Zhang Z, Wang D, Zhou Z, Sun G, Wang S and Sun Y 2018 *Sol. Energy Mater. Sol. Cells* **182** 228
[41] Tajima S, Umehara M, Hasegawa M, Mise T and Itoh T 2017 *Prog. Photovoltaics: Res. Appl.* **25** 14
[42] Li J J, Wang D X, Li X L, Zeng Y and Zhang Y 2018 *Adv. Sci.* **5** 1700744
[43] Duan H S, Yang W, Bob B, Hsu C J, Lei B and Yang Y 2013 *Adv. Funct. Mater.* **23** 1466
[44] Heath J T, Cohen J D and Shafarman W N 2004 *J. Appl. Phys.* **95** 1000
[45] Yan C, Sun K, Huang J, Johnston S, Liu F, Veettil B P, Sun K, Pu A, Zhou F, Stride J A, Green M A and Hao X 2017 *ACS Energy Lett.* **2** 930
[46] Shi J J, Zhnag H Y, Xu X, Li D M, Luo Y H and Meng Q B 2016 *Rev. Sci. Instrum.* **87** 123107
[47] Zhu H, Kalkan A K, Hou J and Fonash S J 1999 *AIP Conf. Proc.* **462** 309
[48] Yan Y, Jiang C S, Noufi R, Wei S H, Moutinho H R and Al-Jassim M M 2007 *Phys. Rev. Lett.* **99** 235504
[49] Li J W, Mitzi D B and Shenoy V B 2011 *ACS Nano* **5** 8613
[50] Yin W J, Wu Y, Wei S H, Noufi R, Al-Jassim M M and Yan Y 2014 *Adv. Energy Mater.* **4** 1300712
[51] Sun L, He J, Kong H, Yue F, Yang P and Chu J 2011 *Sol. Energy Mater. Sol. Cells* **95** 2907
[52] Ito H, Oka M, Ogino T, Takeda A and Mizushima Y 1984 *Jpn. J. Appl. Phys. Part 1 - Regul. Paper Short Notes Rev. Paper* **23** 719